International Journal of Engineering and Technology Innovation, vol. 16, no. 4, 2026, pp. 512-525

Dynamic Shear Response and Shear Failure Mechanism of RC Columns under Lateral Soft Impact

Zhen Tao[1], Fei-Fan Feng[1,2,*], Lin Chen[1], Tao Liu[1], Xian-Zhong Xie[1],
Dong-Jie Shen[3], Hyeon-Jong Hwang[4]

[1]School of Civil Engineering, Hunan University of Science and Technology, Xiangtan, China
[2]Hunan University of Science and Technology Engineering Testing Co., Ltd., Xiangtan, China
[3]School of Civil Engineering, Changsha Vocational & Technical College, Changsha, China
[4]Department of Architecture and Architectural Engineering, Seoul National University, Seoul, Republic of Korea

Received 22 August 2026; revised 22 September 2026; accepted 24 September 2026
DOI: https://doi.org/10.46604/ijeti.2026.16724

Abstract

This study aims to investigate the dynamic shear response and damage mechanisms of reinforced concrete (RC) columns under soft impact. High-fidelity finite element (FE) models are developed and validated against pendulum impact tests, followed by simulations. The results show that, unlike a hard impactor, a soft impactor absorbs kinetic energy through its deformation, which mitigates the dynamic effect and thus decreases the probability of one-way/punching shear failure in RC columns. Dynamic shear force in RC columns increases with increasing impactor stiffness under low-velocity impact, but decreases beyond a critical stiffness under high-velocity impact. This trend results from the transition from one-way shear to punching shear. The inertial force of shear plug is mainly affected by impactor stiffness and impact velocity, whereas other factors exert negligible influence. The punching shear resistance model proposed for hard impact demonstrates good applicability for evaluating the one-way/punching shear failure of RC columns under soft impact.

Keywords: RC columns, soft impact, impactor stiffness, shear resistance mechanism, finite element simulation

1. Introduction

As critical vertical components of both building and bridge structures, reinforced concrete (RC) columns may be subjected to extreme impact loading throughout their design life. Lateral impact induced by rockfalls [1-2], vehicle collisions [3-4], and vessel collisions [5-6] can trigger catastrophic structural failures, such as the collapse of bridge spans and progressive collapse of building structures. Numerous accidents and investigations have shown that RC columns are prone to shear failure under lateral impact loads. Therefore, a systematic investigation of the impact resistance of RC columns is needed to support more reliable design and performance assessment of such members under lateral impact.

In general, the impact response of RC columns is governed by the energy dissipation capacities of both the impacting object and the column itself [7]. Based on the deformation characteristics of the impactor, impact scenarios are broadly categorized into hard and soft impacts. To date, extensive research—including experimental [8–11], numerical [12–14], and theoretical studies [15–18]—has been devoted to the dynamic behavior and failure modes of RC members under hard impact. In such scenarios, the impactor is substantially stiffer than the structural component, and consequently, the bulk of the initial

* Corresponding author. E-mail address: fengfeifan@hnust.edu.cn

kinetic energy is absorbed by the impacted member [10]. Under these conditions, the impact force typically attains its peak within an extremely short duration [13], with both structural inertial effects and material strain-rate effects playing a pronounced role. Moreover, punching shear failure is highly likely to develop in the vicinity of the impact point [16, 18].

Impact involves interaction between the impactor and structural components. In most cases, the impactor can dissipate kinetic energy via self-deformation during collision, as occurs in vehicle and vessel collisions, making soft impact scenarios relatively common in practice [19-21]. When the ratio of impact duration to the natural vibration period of the component is sufficiently small, the structural responses are dominated by stress wave propagation and inertial forces [18]. In contrast, when the ratio is relatively large, components exhibit quasi-static behavior governed by global structural stiffness [22]. Overall, compared with hard impact, there are relatively fewer studies on soft impact at present. The dynamic shear mechanism of RC columns under soft impact remains unclear, particularly the influence of the impactor stiffness on the dynamic shear response and stress mechanism of RC columns. Previous studies have shown that the stiffness of impactors can vary over a wide range in practical applications [23]. Therefore, considering the complexity of the impact issue, it is necessary to conduct in-depth research on the dynamic response and shear failure mechanism of RC columns under soft impact.

In this study, a high-fidelity soft impact FE model consisting of "mass block-spring-rigid massless surface" was established based on the LS-DYNA software. By comparing the impact force time history curve, impact point displacement time history curve, and failure mode under each stiffness condition with those of the existing pendulum impact model, the critical equivalent spring stiffness was determined. Based on this, the dynamic shear response and failure mechanism of RC columns with a small shear span-to-depth ratio under soft impact were systematically studied. Furthermore, the effects of impactor stiffness, impact velocity, impact height (i.e., shear span-to-depth ratio), boundary conditions, and axial compression ratio on the dynamic shear response and damage failure mechanism of RC columns were also investigated. Finally, by comparing the failure modes of the models and the ratio of the peak impact force to the punching shear resistance, the applicability of the proposed punching shear resistance method for distinguishing between one-way and punching shear failure modes of RC columns in soft impact scenarios was evaluated.

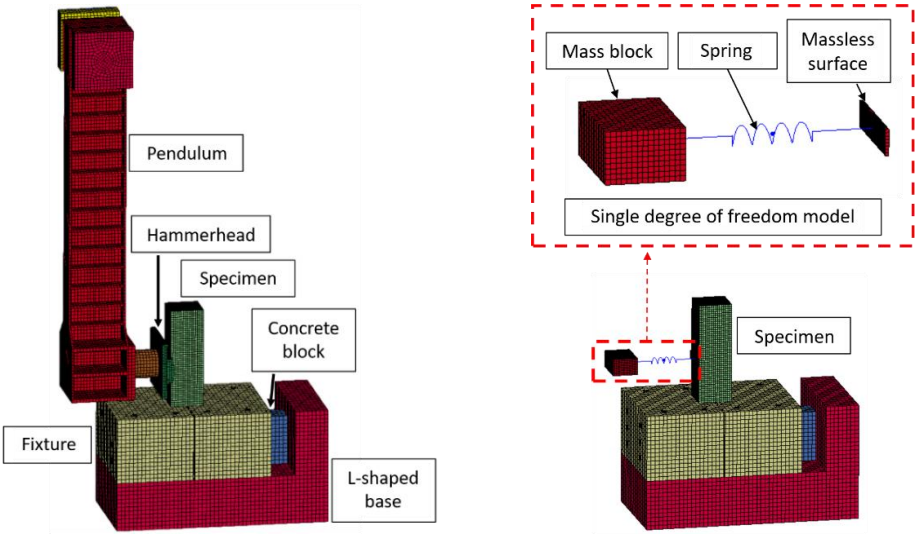
2. FE Modeling of RC Columns under Soft Impact

2.1 Overview of pendulum impact tests and corresponding FE models

The present work is based on previously conducted pendulum impact tests on six quarter-scale square RC columns to study their lateral impact resistance [24]. All specimens have identical dimensions of (200 × 200 × 1000 mm). The six specimens fall into three reinforcement configurations: the standard group (C1, C4, C5, C6), a specimen with thinner longitudinal bars (C2), and a specimen lacking transverse stirrups (C3). Key test variables include shear span-to-depth ratio and impact velocity: 1) Two impact heights (250 and 350 mm) correspond to span-to-depth ratios of 1.4 and 2.0, respectively; and 2) Three pendulum lifting angles (60°, 75°, and 90°) generate impact velocities of 4.90 m/s, 5.68 m/s, and 6.92 m/s, respectively. The pendulum device comprises three subsystems: a loading system, a fixing system, and a supporting system. Full details of the experimental program and loading rig are reported in [24].

To fully understand the dynamic response and shear damage mechanism of RC columns with small shear span-to-depth ratio under pendulum impact, the authors further conducted further numerical studies using the LS-DYNA software [18]. Numerical models corresponding to specimens C1-C6 were established and validated against pendulum impact tests. Fig. 1(a) shows the FE model of the pendulum impact test, in which the concrete was modeled using three-dimensional hexahedral solid elements (SOLID164) with reduced integration, and the rebar was modeled using 2-node Hughes-Liu beam elements (BEAM161) with 2 × 2 Gauss quadrature integration [18]. All components outside the concrete and rebars, namely the pendulum, fixture, concrete block, and L-shaped base, were discretized with eight-node hexahedral solid elements (SOLID164).

At the same time, the anchor bolts were represented by truss beam elements (BEAM161). The mesh size of the specimens was approximately 10 mm according to the mesh sensitivity analysis, while the other parts of the model used a relatively larger mesh size of 25 mm to achieve a favorable trade-off between computational cost and predictive accuracy.



(a) FE model of pendulum impact [18] (b) FE model of soft impact

Fig. 1 Numerical analysis models of hard and soft impacts

The mechanical behavior of concrete under lateral impact is simulated using the continuous surface cap model (CSCM) [13, 23]. The reinforcing bars are described by the bilinear elastic-plastic model *MAT_PLASTIC_KINEMATIC. The rate sensitivity of the rebars is represented by the Cowper-Symonds law, using D = 40.4 and P = 5.0 as the calibrated constants [25, 26]. Except for the concrete and rebars in the specimens, the pendulum, fixture, anchor bolts, base, and concrete block are all modeled using a linear elastic material model by keyword *MAT_ELASTIC. The material parameters (i.e., density, elastic modulus, and Poisson's ratio) of the pendulum, fixture, anchor bolts, and base are all based on standard steel.

For simplicity, only the rotating mechanism, pendulum arm, and hammer head are retained in the simplified numerical model. Given the high stiffness of the steel base and reaction wall, these components are integrated into a unified L-shaped base. Full displacement constraint is applied to the L-shaped base via the keyword *BOUNDARY_SPC_SET to achieve fixed boundary conditions. All interfaces between the hammerhead, specimen, fixture, L-shaped base, and support block are handled by *CONTACT_AUTOMATIC_SURFACE_TO_SURFACE, with a friction coefficient of 0.3 for both static and dynamic contact [26]. Perfect bonding between the rebar and concrete is presumed in the model [27, 28]. Detailed information on the FE model of the pendulum impact tests and its verification can be found in the literature [18].

2.2 Establishment of soft impact FE model

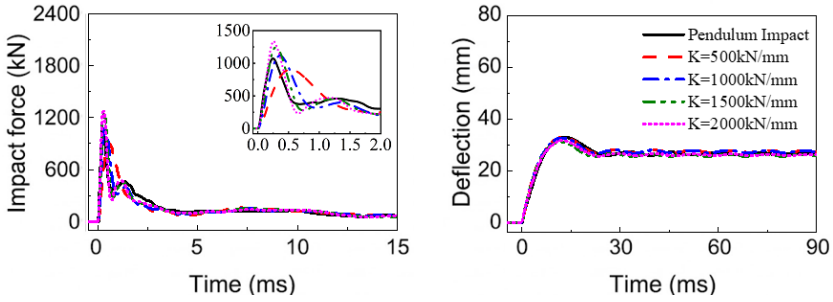
To investigate the influence of impactor stiffness on the dynamic shear response and force mechanism of RC columns under lateral impact, based on the modeling method and parameter values of the FE model in Section 2.1, a soft impact FE model was established in this study (Fig. 1(b)). For simplicity, a single degree-of-freedom model is adopted to simulate the soft impactor [23]. The RC column, fixture, concrete block, and L-shaped base remain unchanged from those in the pendulum impact model. The single degree-of-freedom model consists of a mass block, a linear elastic spring, and a rigid massless surface [23]. The rigid massless surface represents the contact interface between the impactor and the RC column, the mass block represents the impactor mass, and the spring simulates the soft impact behavior.

The mass block and rigid massless surface in the model are modeled using three-dimensional eight-node hexahedral solid elements (SOLID164), while the spring is modeled using the discrete element. The mass block and rigid massless surface in the model are simulated using the rigid material MAT_020 (MAT_RIGID), and the linear elastic spring is modeled using the

elastic spring material MAT_S01 (MAT_SPRING_ELASTIC). The soft impact behavior is controlled by the spring stiffness parameters. Given the complexity of the impact mechanism, the initial kinetic energy and impactor stiffness significantly affect the dynamic response of RC columns under lateral impact. Thus, the density parameter of the mass block (with volume = 220×150×100 mm) is determined by comparing the impact energy under the rigid pendulum impact at an impact velocity of 7 m/s [18] with the soft impact in this study. This procedure ensures energy equivalence between the two impact conditions. On this basis, the critical equivalent spring stiffness of the soft impact is further determined in Section 2.3. The calibrated model is then used for the subsequent parametric analysis that considers a series of parameters, including the impactor stiffness, impact velocity, impact height, boundary conditions, and the axial compression ratio.

2.3 Determination of critical equivalent spring stiffness of soft impact

To accurately calibrate the critical equivalent spring stiffness of the soft impact model for simulating pendulum impact, the single degree-of-freedom model with a mass of 314.21 kg was used to impact an RC column at a velocity of 7 m/s, with an impact height of 250 mm. Four different spring stiffnesses (500, 1000, 1500, and 2000 kN/mm) were selected for comparison with pendulum impact conditions. By comparing the impact force time history curve, the displacement time history curve of the impact point, as well as the damage and failure modes under each condition, the critical equivalent spring stiffness for pendulum impact was determined.



(a) Impact force time histories (b) Deflection time histories

Fig. 2 Comparison of impact force and deflection time histories

Fig. 2(a) compares the impact force time histories for each stiffness level with the pendulum impact. When the impactor stiffness was 500 kN/mm, the impact force was sustained for a longer period with a smaller peak value, and the peak value appeared significantly later; when the stiffness increased to 1000 kN/mm, the impact duration was significantly shortened, and the peak value of the impact force was closer to that of the pendulum impact with a minimum error of 8.59%; when the stiffness further increased to 1500 and 2000 kN/mm, the peak value of the impact force further increased and gradually showed a converging trend, indicating that the impactor approached infinite rigidity at this point. Fig. 2(b) compares the displacement time histories of the impact point under different stiffness levels with the pendulum impact. When the stiffness was 1000 kN/mm, the displacement time response of the impact point was in good agreement with the pendulum impact, with a small error of 0.82%. The corresponding damage and failure modes are presented in Fig. 3.

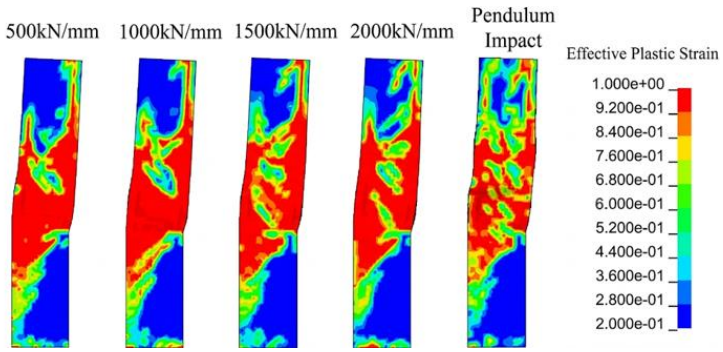


Fig. 3 Comparison of damage and failure modes of RC columns

Fig. 3 compares the damage and failure modes of the RC column in accordance with the spring stiffness level. Since the stiffness of the four impactor cases is relatively large, the stiffness of the impactor has a marginal influence on the damage and failure mode of the RC column. All RC column specimens showed obvious one-way shear failure, and the damage mode was basically consistent with that of the pendulum impact.

In summary, by comparing the impact force time history curve, impact point displacement time history curve, and failure mode under each stiffness condition with those of the pendulum impact, the critical equivalent spring stiffness corresponding to the pendulum impact condition was determined to be 1000 kN/mm. Based on this equivalent spring stiffness, further research will be conducted to investigate the influence of the impactor stiffness on the dynamic shear response and force mechanism of the RC column under lateral impact. It is worth noting that since the pendulum impact model has been rigorously verified against previous physical experiments [18], the critical equivalent spring stiffness of the soft impact model obtained on this basis is reliable and persuasive.

2.4 Dynamic force extraction and parametric matrix

The primary objective of this study is to investigate the shear response and failure mechanisms of RC columns under soft impact, with a specific interest in the transition between one-way shear and punching shear failure. Therefore, two inclined planes at 45° are introduced through *DATABASE_CROSS_SECTION_PLANE to monitor the internal shear forces. The column region bounded by these planes is taken as the shear plug [16] (see Fig. 4). Fig. 4 illustrates how the horizontal shear resisted by the upper and lower inclined sections is decomposed into the individual contributions of concrete, stirrups, and longitudinal bars. More detailed definitions of upper/lower section forces, dynamic shear force, and the inertial force of the shear plug can be found in the literature [18].

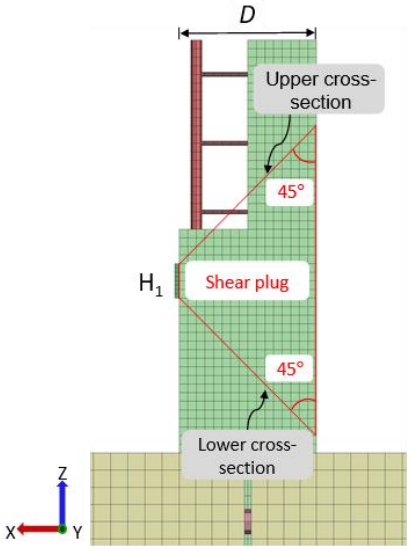


Fig. 4 Schematic diagram of shear plug within RC column

Using the aforementioned benchmark model, this study systematically investigated the effects of various key parameters, such as the impactor stiffness (i.e., 1, 10, 100, or 1000 kN/mm), impact velocity (i.e., 7, 16, or 24 m/s), impact height (i.e., 250, 350, or 450 mm), boundary conditions (i.e., fixed-released, fixed-pinned, or fixed-fixed), and axial compression ratio (i.e., 0.1, 0.2, or 0.3), on the dynamic shear response and damage mechanism of RC columns under lateral impact. Based on the determined equivalent spring stiffness of 1000 kN/mm, four stiffness levels were selected for a parametric study, which basically covers the entire stiffness range from soft impact to hard impact. According to the evolution law of the damage and failure mode of RC columns under the previous pendulum impact conditions, three typical impact velocities (i.e., 7, 16, and 24 m/s) were selected, in which the typical one-way shear failure mode, transition mode from one-way shear to punching shear failure, and punching shear failure mode were exhibited [18]. Table 1 lists the specific parameter conditions for ten series.

Table 1 Impact parameters of reinforced concrete columns

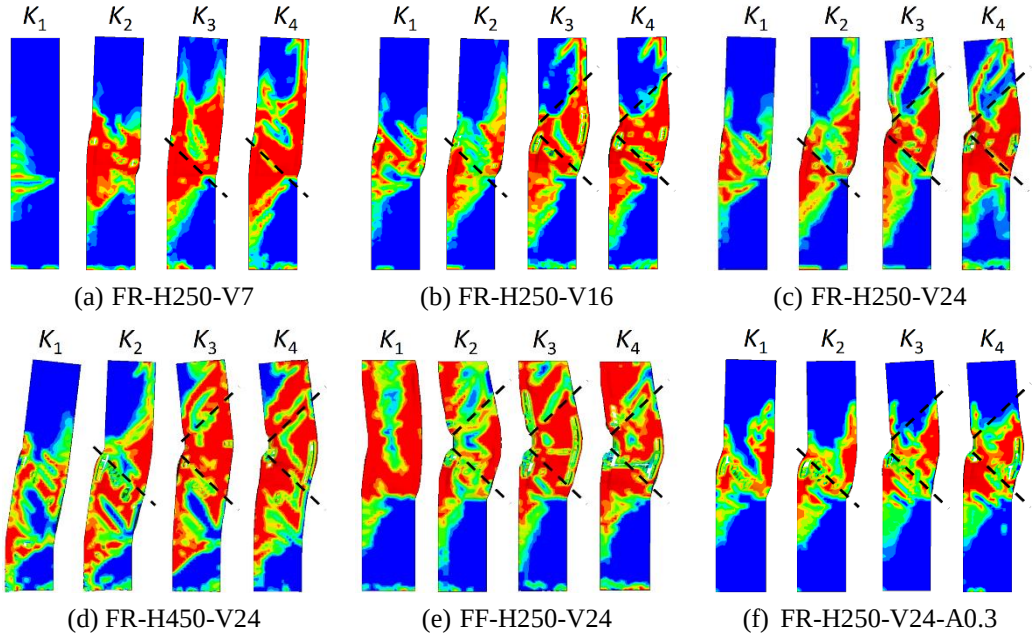
Series	Impactor stiffness (kN/mm)	Impact velocity (m/s)	Impact height (mm)	Boundary conditions	Axial compression ratio
FR-H250-V7 (Series I)	1, 10, 100, 1000	7	250	Fixed-Released	0
FR-H250-V16 (Series II)	1, 10, 100, 1000	16	250	Fixed-Released	0
FR-H250-V24 (Series III)	1, 10, 100, 1000	24	250	Fixed-Released	0
FR-H350-V24 (Series IV)	1, 10, 100, 1000	24	350	Fixed-Released	0
FR-H450-V24 (Series V)	1, 10, 100, 1000	24	450	Fixed-Released	0
FP-H250-V24 (Series VI)	1, 10, 100, 1000	24	250	Fixed-Pinned	0
FF-H250-V24 (Series VII)	1, 10, 100, 1000	24	250	Fixed-Fixed	0
FR-H250-V24-A0.1 (Series VIII)	1, 10, 100, 1000	24	250	Fixed-Released	0.1
FR-H250-V24-A0.2 (Series IX)	1, 10, 100, 1000	24	250	Fixed-Released	0.2
FR-H250-V24-A0.3 (Series X)	1, 10, 100, 1000	24	250	Fixed-Released	0.3

3. Numerical Analysis Results

3.1 General response characteristics

3.1.1 Damage pattern

Fig. 5(a)-(c) present the damage and failure modes of the three typical series FR-H250-V7, FR-H250-V16, and FR-H250-V24 under different impact velocities and impactor stiffnesses. At a lower impact velocity (V = 7 m/s), the RC column mainly exhibited one-way shear damage. As the stiffness increased, the severity of shear damage gradually increased, eventually leading to one-way shear failure at K = 1000 kN/mm. At the impact velocity of V = 16 m/s, when the impactor stiffness was low, the RC column still experienced mainly one-way shear damage. As the impactor stiffness increased, the failure mode transitioned from one-way shear failure to punching shear failure, and a failure mode similar to a shear plug was formed at K = 1000 kN/mm. At V = 24 m/s, one-way shear failure occurred at K = 1 and 10 kN/mm. When the impactor stiffness increased to K = 100 kN/mm, the failure mode of the RC column changed from one-way shear failure to punching shear failure. As the impactor stiffness further increased to K = 1000 kN/mm, the shear plug within the RC column became more prominent.



(a) FR-H250-V7 (b) FR-H250-V16 (c) FR-H250-V24

(d) FR-H450-V24 (e) FF-H250-V24 (f) FR-H250-V24-A0.3

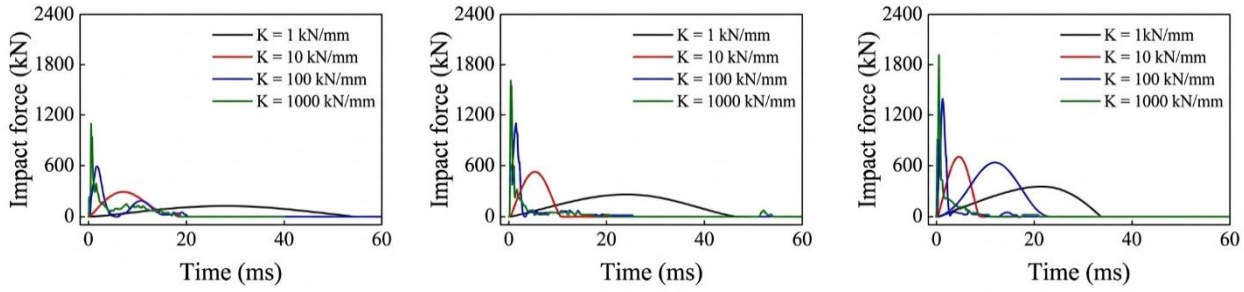
Fig. 5 Failure modes of six typical model series under representative impactor stiffnesses (K1, K2, K3, and K4 = 1, 10, 100, and 1000 kN/mm, respectively)

Fig. 5(d)-(f) further illustrate the damage and failure modes of the other three typical series FR-H450-V24, FF-H250-V24, and FR-H250-V24-A0.3 under different impactor stiffness conditions. As seen in the figures, except for FF-H250-V24, which experienced punching shear failure at a relatively low impactor stiffness due to the fixed end at the column top, both

FR-H450-V24 and FR-H250-V24-A0.3 experienced one-way shear failure at a relatively low impactor stiffness. As a matter of fact, one-way shear failure prevailed in most models at low stiffness levels; however, at K = 1000 kN/mm, all columns except the V7 series developed punching shear failure with a shear plug resembling that in Fig. 4. Under high-velocity impact, as the impactor stiffness increased, the damage mode of the RC column gradually shifted from one-way shear failure to punching shear failure. Moreover, when the impactor stiffness is relatively large (i.e., K = 100 or 1000 kN/mm), the impact height, boundary conditions, and axial compression ratio have limited effects on the damage and failure mode of RC columns.

3.1.2 Dynamic force time histories

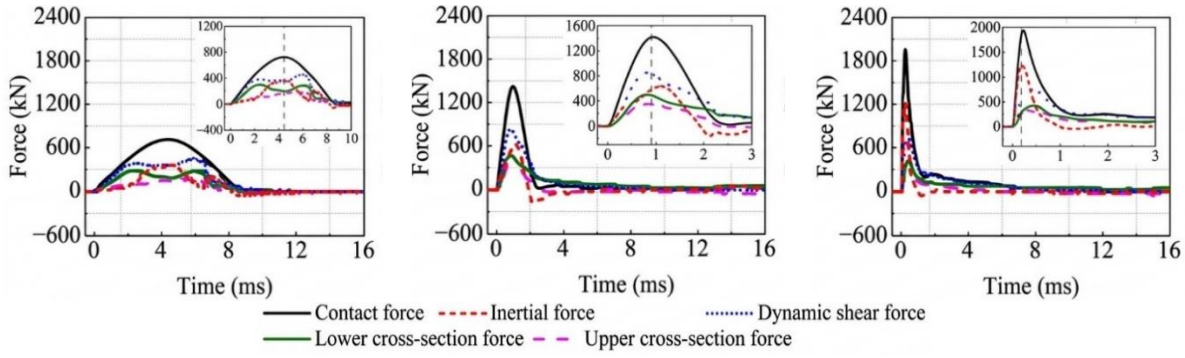
Fig. 6 shows the influence of different impactor stiffnesses on the impact force time histories of the FR-H250 series under three typical impact velocities. At each impact velocity, as the impactor stiffness increased, the peak impact force increased, and the peak force appeared earlier, with the impact force duration shortening. As the impact velocity increased from 7 m/s to 24 m/s, the peak impact force further increased for specimens with the same impactor stiffness. In general, as the impactor stiffness and impact velocity increased, the peak impact force increased, the peak impact force appeared earlier, and the duration of the impact force shortened, which was consistent with the fundamental principles of structural dynamics.



(a) FR-H250-V7 (b) FR-H250-V16 (c) FR-H250-V24

Fig. 6 Impact force time histories of FR-H250 series under different impactor stiffness

Fig. 7 compares the dynamic force variations, including the impact force, dynamic shear force, upper and lower inclined section forces, and inertial force of the shear plug (see Fig. 4) in FR-H250-V24 with typical impactor stiffnesses (K = 10, 100, and 1000 kN/mm). In each subgraph, a vertical dashed line indicates the time corresponding to the peak impact force. As the impactor became stiffer, both the impact force and the inertial force grew, and the instants at which these forces and the dynamic shear force peaked converged. In particular, as the impactor stiffness increased, the inertial force closely followed the impact force in the initial stage, indicating an increasingly pronounced dynamic effect in the column. It is worth noting that, compared to crack patterns and failure modes, the evolution of the dynamic shear forces on the upper and lower sections of the shear plug provides a more direct basis for identifying one-way shear failure and punching shear failure. For a detailed discussion on this issue, please refer to reference [18].



(a) FR-H250-V24-K10 (b) FR-H250-V24-K100 (c) FR-H250-V24-K1000

Fig. 7 Time histories of dynamic forces acting on FR-H250-V24 under different impactor stiffnesses

3.2 Dynamic shear force and its components

3.2.1 Peaks of total dynamic shear force

To understand how RC columns resist shear under soft impact, the evolution and composition of their dynamic shear force need to be examined in detail. Fig. 8 plots the peak dynamic shear force of the RC column against the key parameters considered. In general, under low-velocity impact (V = 7 m/s), the peak dynamic shear force of the column increased with increasing impactor stiffness, and the shear damage of the column also gradually intensified, eventually leading to one-way shear failure (see Fig. 5(a)). In contrast, in high-velocity impact, as the impactor stiffness increased, the peak dynamic shear force increased and then decreased. This phenomenon is associated with the transformation of the failure mode from one-way shear failure to punching shear failure (see Fig. 5(b)-(f)). According to the author's previous study [18], when the specimen was governed by punching shear failure under pendulum impact, the forces of the upper and lower sections of the column reached their peak in the local response stage, and the corresponding peak dynamic shear force at this time was less than the peak dynamic shear force corresponding to one-way shear failure in the global response stage. Regarding the two-stage response characteristics and their divisions, please refer to the literature [18].

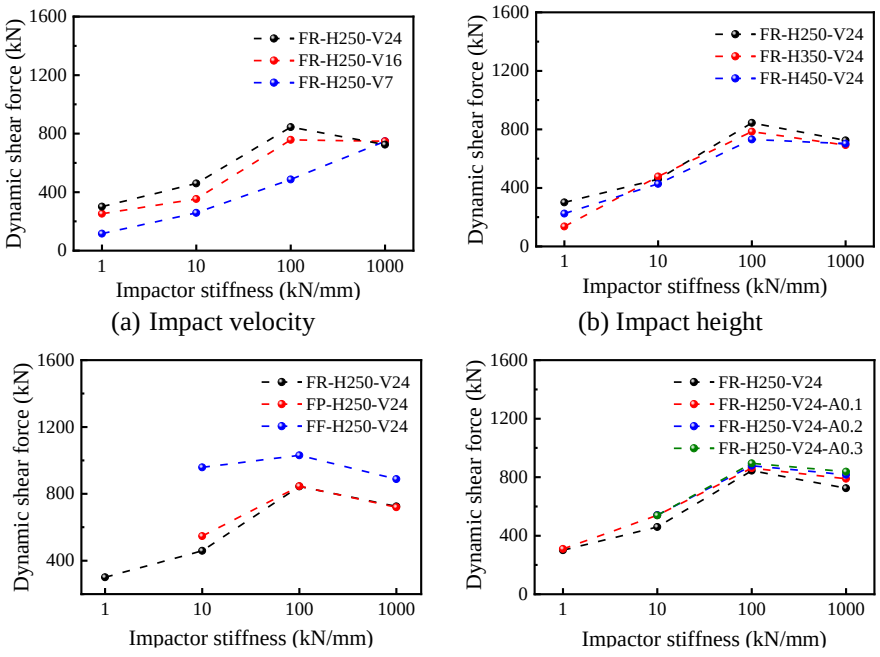


Fig. 8 Variation of the dynamic shear force with impactor stiffness for each simulation series

As shown in Fig. 8(a), at low stiffness, the peak dynamic shear force showed an upward trend as the impact velocity increased. However, when the stiffness reaches K = 1000 kN/mm, an increase in impact velocity no longer leads to an increase in the peak dynamic shear force. This is because the column undergoes punching shear failure under high-velocity and high-stiffness impact (see Fig. 5(c)). The impact height has some effect on the dynamic shear force of RC columns at lower impactor stiffness. (Fig. 8(b)). However, when the impactor stiffness reached K = 1000 kN/mm, the influence of impact height became negligible. This behavior is also associated with the transition to punching shear failure under high-velocity and high-stiffness impact (see Fig. 5(d)).

When the boundary condition changed from FR (or FP) to FF, the peak dynamic shear force significantly increased (Fig. 8(c)), because the fixed constraint at both ends of the RC column generated a significant arching effect. In addition, when the impactor stiffness reached K = 1000 kN/mm, the influence of boundary conditions became smaller due to the transition from one-way shear to punching shear failure. The coupling effect of the arching action and the impactor stiffness on the peak dynamic shear force is worthy of further investigation. As shown in Fig. 8(d), an increase in the axial compression ratio

increased the peak dynamic shear force of the column to some extent. When the impact stiffness increased from K = 100 kN/mm to 1000 kN/mm, the change in the axial compression ratio became more sensitive to the peak dynamic shear force. The coupling influence of axial compression and impactor stiffness on the peak dynamic shear force merits further study.

3.2.2 Composition of dynamic shear force

Fig. 9 breaks down the shear resisted by series III-X columns at the peak impact force under a 1000 kN/mm impactor, when every column failed in punching shear (Fig. 5). In all cases, the concrete contribution was the highest, accounting for more than 90% of the total dynamic shear force, while the longitudinal reinforcement and stirrups contributed to the remaining 4-6% and 2-3%, respectively. The longitudinal reinforcement therefore provided a greater shear resistance compared to the stirrups, which was consistent with the author's previous research results. That is, when the impact force reached its peak, due to the very short action time, the structural deformation was still very small. At this time, the punching damage had not yet fully occurred, resulting in the stirrups being unable to fully perform their function [18]. Another point that deserves special attention is that as the structural deformation increases, the contributions of the three components change dynamically. From then on, the proportion of the rebar's contribution will increase, while that of the concrete will decrease.

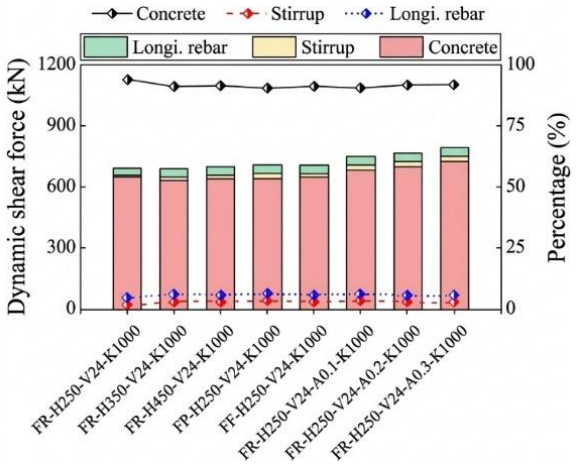
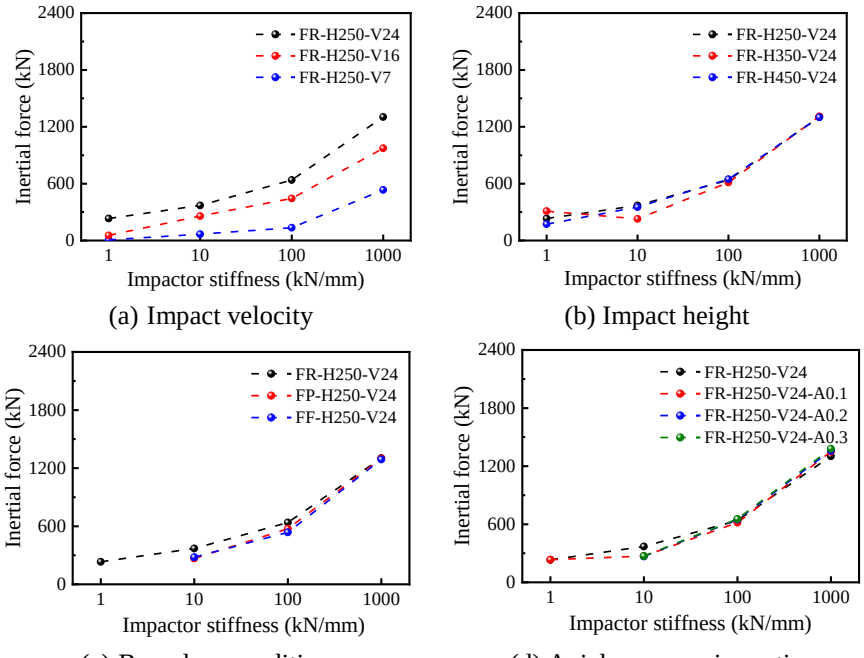


Fig. 9 Components of the shear force in RC columns at peak impact under a 1000 kN/mm impactor

3.3 Inertial force of shear plug



(a) Impact velocity (b) Impact height

(c) Boundary conditions (d) Axial compression ratio

Fig. 10 Relationship between peak inertial force and impactor stiffness

Together with strain-rate sensitivity, the inertial effect is responsible for the pronounced difference between the impact and static responses of RC columns. Fig. 10 presents the peak inertial force of the shear plug under the various parameters. In general, as the impactor stiffness increased, the peak inertial force increased. At the same impactor stiffness, it also increased with increasing impact velocity (Fig. 10(a)). In contrast, the impact height, boundary conditions, and axial compression ratio, etc., had relatively limited influence on the peak inertial force of the shear plug. This finding is also consistent with the previous research conclusion on the inertial force of the shear plug under pendulum impact. The study showed that, without considering the influence of the impactor stiffness, the main factors affecting the peak inertial force of the shear plug are the impact velocity and the cross-sectional size of the column. In contrast, other factors have little impact [18].

4. Failure Mode Evaluation of RC Column under Soft Impact

A large number of studies have shown that RC components are highly prone to one-way/punching shear failure under impact loading. Previously, Do et al. [16] proposed a calculation formula for the punching shear resistance of RC columns, indicating that when the peak impact force exceeds the punching shear resistance P_{dyn}^{max}, the RC column is expected to develop shear failure on the two inclined sections at 45° away from the impact area (i.e., punching shear failure). When the peak impact force falls between $0.5P_{dyn}^{max}$ and P_{dyn}^{max}, one-way shear failure will occur within the shear span area of the column. Research has shown that this calculation formula can effectively evaluate the one-way/punching shear failure of RC columns.

However, the calculation formula only includes variables related to the tensile strength of concrete and the cross-sectional size of columns. The inertia effect and the contribution of steel bars are implicitly taken into account in the dimensionless coefficient KT, without clearly distinguishing the two-stage response of RC columns under impact, namely the local response stage corresponding to punching shear failure and the global response stage corresponding to one-way shear failure. Based on the method proposed by Do et al. [16], the authors further modified the formula for calculating the punching shear resistance, as expressed below, which explicitly considered the influence of inertia effects to evaluate the shear failure mode of RC columns based on the magnitude of the peak impact force and P_{dyn}^{max} [18]:

$$P_{dyn}^{max} = P_c + P_I \tag{1}$$

$$P_c = 3.56 \times f_t \times W \times D \tag{2}$$

$$P_I = 0.439 \times PIF + 0.00344 \times \frac{PIF^2}{\rho_c \times (D + H_I) \times D \times W} \tag{3}$$

where P_c represents the resistance furnished by the column, P_I represents the resistance furnished by the inertial force, f_t represents the tensile strength of concrete, and W and D denote the cross-sectional width and depth, respectively; ρ_c is taken as the density of concrete (2400 kg/ m^3) for simplicity, and H_I is the height of the contact zone between the hammerhead and specimens (i.e., 50 mm in this study).

To evaluate the accuracy and applicability of the proposed punching shear resistance in predicting the failure modes of RC columns under soft impact, the results of a total of 40 models across ten series in this study and 8 numerical cases from existing literature [23] were compared and evaluated. Fig. 11 shows the relationship between the failure mode of the RC column and the ratio of peak impact force to P_{dyn}^{max}, while Table 2 summarizes the corresponding calculation results. The proposed method showed a high degree of consistency with the model's failure mode. For all cases where punching shear failure occurred, the PIF/P_{dyn}^{max} ratio was around 1.0, while for cases without punching shear failure, the ratio was below 1.0.

For Series I, due to the relatively low impact velocity (7 m/s), even when the stiffness was relatively large (K = 1000 kN/mm), the RC column only exhibited one-way shear failure. At this time, the maximum PIF/P_{dyn}^{max} ratio was 0.94, which was in good agreement with the final failure mode (see Fig. 5(a)). For Series II under the impact velocity of 16 m/s, when the impactor stiffness was low (K = 1 and 10 kN/mm), the RC column exhibited one-way shear damage and failure (see Fig. 5(b)),

with PIF/P_{dyn}^{max} ratios of 0.41 and 0.68, respectively. When the impactor stiffness increased to K = 100 kN/mm, the PIF/P_{dyn}^{max} ratio reached 0.94, indicating a transition from one-way shear failure to punching shear failure. When the impactor stiffness was further increased to K = 1000 kN/mm, the RC column exhibited punching shear failure, with a PIF/P_{dyn}^{max} ratio of 1.01.

For the series III to X under higher impact velocities, when the impactor stiffness was relatively low (K = 1 and 10 kN/mm), the PIF/P_{dyn}^{max} values were all less than 1.0, which was in good agreement with the one-way shear failure mode of the specimens. When the impactor stiffness increased to K = 100 kN/mm or above, the specimens experienced punching shear failure (see Fig. 5(c)-(f)). At this time, the PIF/P_{dyn}^{max} values were between 0.99 and 1.02, indicating the accuracy of the proposed calculation formula for punching shear resistance. Besides, for the series XI to XII [23] with different impact velocities and impactor stiffnesses, due to the relatively low stiffness of the impactor, all specimens experienced one-way shear failure with the PIF/P_{dyn}^{max} values not exceeding 0.67, which further indicates the accuracy and reliability of the proposed calculation formula.

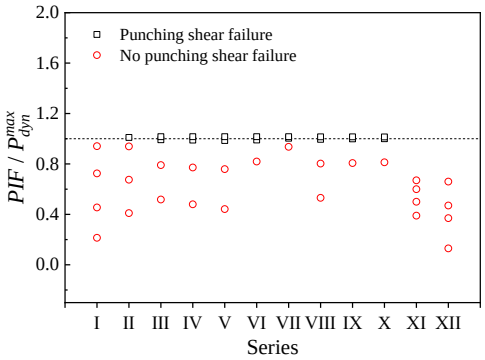


Fig. 11 Relationship between damage level of RC columns and the PIF/P_{dyn}^{max} ratio for every series

Table 2 Evaluation of one-way/punching shear failure of RC columns under soft impact

Series	Impactor stiffness (kN/mm)	PIF (kN)	P_{dyn}^{max} (kN)	PIF/P_{dyn}^{max}	Punching shear failure
FR-H250-V7 (Series I)	1	123.022	574.5	0.21	No
	10	302.001	664.0	0.45	No
	100	607.098	837.6	0.72	No
	1000	1120	1189.8	0.94	No
FR-H250-V16 (Series II)	1	263.936	644.2	0.41	No
	10	537	795.4	0.68	No
	100	1110.15	1182.3	0.94	No
	1000	1631.7	1616.2	1.01	Yes
FR-H250-V24 (Series III)	1	359.53	694.7	0.52	No
	10	718.004	907.4	0.79	No
	100	1414.67	1426.2	0.99	Yes
	1000	1927.59	1897.1	1.02	Yes
FR-H350-V24 (Series IV)	1	324	675.6	0.48	No
	10	683	885.0	0.77	No
	100	1390	1405.4	0.99	Yes
	1000	1890	1860.0	1.02	Yes
FR-H450-V24 (Series V)	1	291	658.2	0.44	No
	10	662	871.7	0.76	No
	100	1370	1388.8	0.99	Yes
	1000	1900	1869.8	1.02	Yes
FP-H250-V24 (Series VI)	1	N/A	N/A	N/A	No
	10	773	943.3	0.82	No
	100	1383.52	1400.0	0.99	Yes
	1000	1900	1869.8	1.02	Yes
FF-H250-V24 (Series VII)	1	N/A	N/A	N/A	No
	10	1100	1174.6	0.94	No
	100	1550	1543.1	1.00	Yes
	1000	1910	1879.7	1.02	Yes

Table 2 Evaluation of one-way/punching shear failure of RC columns under soft impact (continued)

Series	Impactor stiffness (kN/mm)	*PIF* (kN)	P_{dyn}^{max} (kN)	PIF/P_{dyn}^{max}	Punching shear failure
FR-H250-V24-A0.1 (Series VIII)	1	373	702.0	0.53	No
	10	741	922.3	0.80	No
	100	1440	1447.7	0.99	Yes
	1000	2020	1989.9	1.02	Yes
FR-H250-V24-A0.2 (Series IX)	1	N/A	N/A	N/A	No
	10	748	926.9	0.81	No
	100	1480	1482.0	1.00	Yes
	1000	2010	1979.8	1.02	Yes
FR-H250-V24-A0.3 (Series X)	1	N/A	N/A	N/A	No
	10	759	934.1	0.81	No
	100	1500	1499.3	1.00	Yes
	1000	2060	2030.9	1.01	Yes
C400-M2.0-V15-N0.3-h1.0 (Series XI) Zhao et al. [23]	2	943	2425.3	0.39	No
	4	1302	2598.9	0.50	No
	8	1655	2774.7	0.60	No
	16	1967	2934.1	0.67	No
C400-M2.0-V10-N0.3-h1.0 (Series XII) Zhao et al. [23]	0.4	281	2118.5	0.13	No
	4	882	2396.3	0.37	No
	8	1211	2554.4	0.47	No
	40	1934	2917.1	0.66	No

Note: N/A indicates that under this condition, a secondary impact caused by the mass block occurred due to the spring stiffness being too small, which is beyond the scope of this study.

In summary, comparison of the observed failure mode with the ratio of the peak impact force to the punching shear resistance indicates that the punching shear resistance formulation proposed by the authors previously can still accurately predict the one-way/punching shear failure mode of RC columns under soft impact scenarios.

5. Conclusions

This study employed high-fidelity numerical simulations to examine the dynamic shear response and damage mechanisms of RC columns subjected to soft impact. Based on the calculation formula for punching shear resistance, the applicability of this method in discriminating the one-way/punching shear failure modes of RC columns in soft impact scenarios was also preliminarily evaluated. The main conclusions are summarized as follows:

(1) A simplified single degree-of-freedom model representing soft impact was established in this study. By comparing the impact force time history curve, displacement time history curve, and failure mode of RC columns under different spring stiffnesses, the critical equivalent spring stiffness equivalent to the existing pendulum impact model was determined. On this basis, the calibrated model was used to systematically investigate the dynamic shear response and shear damage mechanism of RC columns under soft impact.

(2) The dynamic response of RC columns under soft impact differs significantly from that under hard impact. During the impact process, the soft impactor first dissipates part of the initial kinetic energy through its own deformation, and the impact force only reaches its peak after a relatively long period of time. When the impactor stiffness is relatively low, due to the weakened dynamic effect of the column, the probability of RC columns experiencing one-way/punching shear failure decreases.

(3) The peak dynamic shear force of RC columns increases as impactor stiffness increases under low-velocity impact. However, under high-velocity impacts, when the impactor stiffness reaches a certain critical threshold, an increase in impactor stiffness leads to a downward trend in the peak dynamic shear force. This is because the failure mode of the column changes from one-way shear failure in the global response stage to punching shear failure in the local response stage. During punching shear failure, the dynamic shear force of the RC column is lower than that of one-way shear failure.

(4) The inertial force of the shear plug of RC columns is mainly related to the impactor stiffness and the impact velocity, whereas impact height, boundary conditions, and axial compression ratio had relatively limited effects. When the impactor stiffness is relatively small, the inertial effect was also limited, and the response of the RC column under soft impact approaches that under static loading.

(5) In soft impact scenarios, by comparing the failure mode of the models with the ratio of the peak impact force to the punching shear resistance, it is shown that the calculation formula of the punching shear resistance previously proposed by the authors can still effectively predict the one-way/punching shear failure mode of RC columns under soft impact, indicating that this assessment method still has good applicability and accuracy in the soft impact scenario.

It should be noted that the impactor stiffness and the impact velocity have a significant coupling effect on the failure mode transition of the RC column, and the critical stiffness corresponding to the failure mode transition is also related to the section characteristics of the RC column. Further studies regarding the specific critical stiffness should be carried out in the future.

Acknowledgement

This work was supported by the Scientific Research Foundation of Education Department of Hunan Province of China (Grant No. 25B0442, 23B1140), the National Natural Science Foundation of China (Grant No. 52278500), the Hunan Provincial Natural Science Foundation of China (Grant No. 2024JJ9066), and the National Research Foundation of Korea (NRF) grant funded by the Korea government (MSIT) (No. RS-2024-00409719). The authors sincerely thank all funding agencies for their support.

Conflicts of Interest

The authors declare no conflict of interest.

References

[1] C. J. Laura, B. F. Elena, and C. F. Daniel, “Design of a New Energy Dissipating Device and Verification for Use in Rockfall Protection Barriers,” Engineering Structures, vol. 199, article no. 109633, 2019.

[2] R. H. Xie, W. Fan, B. Liu, and D. J. Shen, “Dynamic Behavior and Vulnerability Analysis of Bridge Columns with Different Cross-Sectional Shapes under Rockfall Impacts,” Structures, vol. 26, pp. 471-486, 2020.

[3] H. Sharma, S. Hurlebaus, and P. Gardoni, “Performance-Based Response Evaluation of Reinforced Concrete Columns Subject to Vehicle Impact,” International Journal of Impact Engineering, vol. 43, pp. 52-62, 2012.

[4] R. Cao, S. El-Tawil, A. K. Agrawal, X. Xu, and W. Wong, “Behavior and Design of Bridge Piers Subjected to Heavy Truck Collision,” Journal of Bridge Engineering, vol. 24, no. 7, article no. 4019057, 2019.

[5] H. Jiang, J. J. Wang, M. G. Chorzepa, and J. D. Zhao, “Numerical Investigation of Progressive Collapse of a Multispan Continuous Bridge Subjected to Vessel Collision,” Journal of Bridge Engineering, vol. 22, no. 5, article no. 04017008, 2017.

[6] G. Gholipour, C. W. Zhang, and A. A. Mousavi, “Nonlinear Failure Analysis of Bridge Pier Subjected to Vessel Impact Combined with Blast Loads,” Ocean Engineering, vol. 234, article no. 109209, 2021.

[7] J. Louw, G. Maritz, and M. Loedolff, “The Behaviour of RC Columns under Impact Loading,” The Civil Engineer in South Africa, vol. 34, no. 11, pp. 371-378, 1992.

[8] H. W. Li, W. S. Chen, Z. J. Huang, H. Hao, T. T. Ngo, and T. M. Pham, “Influence of Various Impact Scenarios on the Dynamic Performance of Concrete Beam-Column Joints,” International Journal of Impact Engineering, vol. 167, article no. 104284, 2022.

[9] J. M. Sun, W. J. Yi, H. Chen, F. Peng, Y. Zhou, and W. X. Zhang, “Dynamic Responses of RC Columns under Axial Load and Lateral Impact,” Journal of Structural Engineering, vol. 149, no. 1, article no. 04022210, 2023.

[10] D. J. Zhou, L. Chen, C. Demartino, L. P. Li, and T. Liu, “Internal and External Steel-Tube Strengthened RC Columns: Impact Tests and Numerical Simulations,” Journal of Constructional Steel Research, vol. 219, article no. 108752, 2024.

[11] D. B. Zhao, Y. M. Wen, J. M. Sun, H. Xiong, and M. J. Hao, "Lateral-Impact Behavior of Axially Preloaded RC Columns Strengthened with Large-Rupture-Strain FRP Wraps," Journal of Composites for Construction, vol. 28, no. 3, article no. 04024012, 2024.

[12] Z. H. Hou, J. W. Xu, J. M. Sun, F. Luo, and W. Q. Zhao, "Dynamic Response and Shear Mechanisms of Reinforced Concrete Columns Subjected to Lateral Impact," International Journal of Engineering and Technology Innovation, vol. 16, no. 2, pp. 179-198, 2026.

[13] J. M. Sun, H. Chen, F. Yi, Y. B. Ding, Y. Zhou, Q. F. He, et al., "Experimental and Numerical Study on Influence of Impact Mass and Velocity on Failure Mode of RC Columns under Lateral Impact," Engineering Structures, vol. 314, article no. 118416, 2024.

[14] C. Chen, Z. J. Zhang, Y. Y. Tang, L. Zhang, and W. C. Xu, "Numerical Study of Load Transfer in Conventional and X-Shaped Sleeper-Ballast Systems under Impact Loading," Journal of Railway Science and Technology, vol. 2, no. 1, pp. 27-40, 2026.

[15] W. J. Yi, D. B. Zhao, and S. K. Kunnath, "Simplified Approach for Assessing Shear Resistance of Reinforced Concrete Beams under Impact Loads," ACI Structural Journal, vol. 113, no. 4, pp. 747-756, 2016.

[16] T. V. Do, T. M. Pham, and H. Hao, "Impact Force Profile and Failure Classification of Reinforced Concrete Bridge Columns against Vehicle Impact," Engineering Structures, vol. 183, pp. 443-458, 2019.

[17] W. C. Zhao and J. Qian, "Resistance Mechanism and Reliability Analysis of Reinforced Concrete Columns Subjected to Lateral Impact," International Journal of Impact Engineering, vol. 136, article no. 103413, 2020.

[18] F. F. Feng, L. Chen, D. J. Zhou, T. Liu, D. G. Ou, and Y. Lu, "Two-Stage Dynamic Shear Response of Square RC Columns under Lateral Impact: Mechanisms, Inertial Force Analysis, and Punching Shear Resistance Model," Engineering Structures, vol. 338, article no. 120579, 2025.

[19] T. V. Do, T. M. Pham, and H. Hao, "Dynamic Responses and Failure Modes of Bridge Columns under Vehicle Collision," Engineering Structures, vol. 156, pp. 243-259, 2018.

[20] K. Heng, R. Li, Z. Li, and H. Wu, "Dynamic Responses of Highway Bridge Subjected to Heavy Truck Impact," Engineering Structures, vol. 232, article no. 111828, 2021.

[21] W. C. Zhao, J. H. Ye, and J. Qian, "Dynamic Behavior and Damage Mechanisms of Reinforced Concrete Piers Subjected to Truck Impact," Engineering Failure Analysis, vol. 121, article no. 105158, 2021.

[22] H. Hao, "Predictions of Structural Response to Dynamic Loads of Different Loading Rates," International Journal of Protective Structures, vol. 6, no. 4, pp. 585-605, 2015.

[23] W. C. Zhao and J. H. Ye, "Dynamic Behavior and Damage Assessment of RC Columns Subjected to Lateral Soft Impact," Engineering Structures, vol. 251, part A, article no. 113476, 2022.

[24] L. Chen, D. J. Zhou, F. F. Feng, T. Liu, and C. Wu, "Shear Damage Behavior of RC Columns with Small Shear-to-Span Ratios under Lateral Impact and Static Load," China Journal of Highway and Transport, vol. 37, no. 5, pp. 211-221, 2024 (in Chinese).

[25] P. S. Symonds, "Survey of Methods of Analysis for Plastic Deformation of Structures under Dynamic Loading," Ph.D. dissertation, Department of Engineering, Brown University, Providence, RI, 1967.

[26] R. W. Li, X. X. Zheng, and H. Wu, "Influence of Stirrup Ratio on Vehicular Impact Resistance of Double-Column RC Bridge Piers," Engineering Structures, vol. 289, article no. 116309, 2023.

[27] T. V. Do, T. M. Pham, and H. Hao, "Numerical Investigation of the Behavior of Precast Concrete Segmental Columns Subjected to Vehicle Collision," Engineering Structures, vol. 156, pp. 375-393, 2018.

[28] M. Wu, L. Jin, and X. L. Du, "Dynamic Responses and Reliability Analysis of Bridge Double Column under Vehicle Collision," Engineering Structures, vol. 221, article no. 111035, 2020.



Copyright© by the authors. Licensee TAETI, Taiwan. This article is an open access article distributed under the terms and conditions of the Creative Commons Attribution (CC BY-NC) license (https://creativecommons.org/licenses/by-nc/4.0/).